



Impact of heart rate on coronary computed tomographic angiography interpretability with a third-generation dual-source scanner



Robert J.H. Miller^{a,1}, Evann Eisenberg^{a,1}, John Friedman^a, Victor Cheng^b, Sean Hayes^a, Balaji Tamarappoo^a, Louise Thomson^a, Daniel S. Berman^{a,*}

^a Department of Imaging, Medicine, and Biomedical Sciences, Cedars-Sinai Medical Center, Los Angeles, CA, United States

^b Department of Cardiac Imaging, Oklahoma Heart Institute, Tulsa, OK, United States

ARTICLE INFO

Article history:

Received 16 June 2019

Received in revised form 20 July 2019

Accepted 31 July 2019

Available online 4 August 2019

Keywords:

Coronary computed tomographic angiography

Heart rate

Image quality

ABSTRACT

Background: Guidelines suggest coronary computed tomography angiography (CCTA) should be performed with a heart rate (HR) below 60. Third-generation dual-source CT (DSCT) scanners, with improved temporal resolution, and end-systolic acquisition may facilitate imaging at higher HRs. We determined the influence of HR and end-systolic acquisition on image interpretability and quality with a third-generation DSCT.

Methods: Patients who underwent CCTA between July 2017 and December 2018 were retrospectively identified. All images were acquired using a SOMATOM Force scanner (Siemens Healthcare). The primary outcome was the presence of any uninterpretable coronary segment. The association between HR and CCTA with uninterpretable segments was assessed with multivariable logistic regression, correcting for demographics and imaging variables.

Results: In total, 2620 patients were included, mean age 61.4 ± 12.9 years and 61.2% male, with uninterpretable segments present in 229 (8.7%) scans. In multivariable analysis, HR 80–89 was associated with an increased likelihood of having a scan with uninterpretable segments (adjusted odds ratio [OR] 4.53, $p < 0.001$). However, no significant association was present with end-systolic acquisition (HR 80–89, adjusted OR 2.32, $p = 0.125$). HR ≥ 90 was associated with a decreased likelihood of good or excellent image quality (adjusted OR 0.26, 95% CI 0.11–0.63, $p = 0.003$).

Conclusions: With third-generation dual-source CT scanners, patients with HR 60–80 can be imaged without impacting image interpretability. End-systolic image acquisition facilitates imaging at HRs > 80 without increasing non-diagnostic scans. Routine use of systolic gating could omit the need for strict HR control and pre-test beta blockade currently required for CCTA.

© 2019 Elsevier B.V. All rights reserved.

1. Introduction

Coronary computed tomography angiography (CCTA) is the most sensitive non-invasive diagnostic study for detection of coronary artery disease (CAD). In patients who present to the emergency room (ER) with chest pain, CCTA reduces total ER time and hospital costs while safely excluding acute coronary syndrome [1,2]. In patients with suspected CAD, an initial diagnostic strategy utilizing CCTA decreases the incidence of death or non-fatal myocardial infarction (MI) compared to functional testing [3]. With increasing demand for CCTA,

strategies aimed at reducing procedure times and improving patient flow are increasingly important.

Coronary motion is a major source of non-diagnostic coronary segments. At low heart rates (HR), mid-diastole provides a relatively long and predictable motion-free period compared to end-systole. However, when the HR exceeds 65 beats per minute (bpm), motion-free diastole shortens significantly while the end-systolic period remains relatively constant [4]. Motion artifact most often occurs when CT scanner temporal resolution exceeds the motion-free interval. Therefore, current guidelines recommend that patients receive medications prior to CCTA to achieve a HR below 60 bpm [5]. However, these recommendations are based on studies using single-source, first-generation scanners [6,7].

In recent years, third-generation dual-source CT (DSCT) scanners have been developed with gantry rotation times of 250 msec resulting in an effective temporal resolution of 66 msec. This improvement in temporal resolution may permit high-quality CCTA images with prospective-ECG gating at higher HRs, decreasing the need for aggressive HR control prior to scanning and potentially decreasing the need

Abbreviations: CAC, coronary artery calcium; CAD, coronary artery disease; CCTA, coronary computed tomographic angiography; CI, confidence interval; DLP, dose-length product; DSCT, dual source computed tomography; ER, emergency room; HR, heart rate; OR, odds ratio; PCI, percutaneous coronary intervention.

* Corresponding author at: Cedars-Sinai Medical Center, Room 1258, 8700 Beverly Boulevard, Los Angeles, CA 90048, United States.

E-mail address: bermand@cshs.org (D.S. Berman).

¹ Authors contributed equally.

for beta-blockade. Decreasing pre-scan beta-blockade could simplify outpatient preparation, decrease ER wait times, and improve patient flow by decreasing the need for intravenous beta-blockade. We performed a retrospective analysis of patients undergoing CCTA to determine associations between HR and image interpretability using a third-generation DSCT scanner and end-systolic phase reconstructions.

2. Methods

2.1. Study design and population

Patients who underwent CCTA at Cedars-Sinai Medical Center between July 2017 and December 2018 were retrospectively identified. Patients who did not consent to research ($n = 351$) and those with previous coronary artery bypass grafting were excluded ($n = 91$). Patients in whom HR prior to CCTA was not documented were also excluded ($n = 130$).

Demographic information was collected at the time of imaging including age, sex, body mass index (BMI), past medical history (hypertension, diabetes, dyslipidemia, previous myocardial infarction [MI], previous percutaneous coronary intervention [PCI]), and medications. Obesity was defined as a BMI ≥ 30 kg/m². Additionally, HR information prior to CCTA was collected including HR prior to beta-blocker administration, HR at the time of contrast injection, and maximal HR during injection. HR at the time of contrast injection was used to define HR at the time of CCTA and was categorized as <50 , 50–59, 60–69, 70–79, 80–89, and ≥ 90 . HR variability was defined as the difference between HR at time of contrast injection and maximum HR during CCTA acquisitions. Finally, patient location at the time of CCTA was classified as outpatient, inpatient, or ER.

2.2. CT acquisition and processing

All CCTA images were acquired using a 192-slice third-generation DSCT scanner (SOMATOM Force, Siemens Medical Solutions, Forchheim, Germany). Prior to contrast injection, an anterior-posterior topogram was acquired and used to define the field of view for each patient. If indicated, a low-dose non-contrast cardiac CT was performed to calculate a coronary artery calcium (CAC) score [8]. CCTA acquisition was performed with a collimation of $2 \times 192 \times 0.6$ mm and a gantry rotation time of 0.25 s. Automatic exposure control was active, enabling both the adjustment of tube voltage (CAREkV, Siemens) and tube current (CAREdose, Siemens) based on the topogram information. Tube voltage (80–120 kV) and current (300–700 mA) were further adjusted as needed by technologists with >5 years of experience.

Prior to the exam, metoprolol tartrate (50–100 mg orally) was administered to 1696 (64.7%) patients. Over the study period, patients were studied with one of three scanning protocols: prospective ECG-gated sequential acquisition with images acquired during mid-diastole (relative delay of 60–75%); prospective ECG-gated sequential acquisition at end-systole (absolute delay 280–450 ms); or ECG-gated helical acquisition for patients with BMI >35 kg/m² or with atrial fibrillation. For all helical acquisitions, dose modulation was applied, and optimal image acquisition was performed at end-systole or mid-diastole. CCTA protocol and acquisition window were chosen by an experienced technician after consideration of institutional guidelines which include age, HR, the presence of arrhythmia, obesity, and chest diameter. Studies were excluded if both mid-diastole and end-systole were reconstructed for clinical reading ($n = 44$).

Scans were initiated using automatic bolus tracking with a region of interest (ROI) placed in the ascending aorta, automatically starting acquisition 8 s after reaching a preset attenuation threshold of 100 Hounsfield units (HU). All scans were performed using a single inspiratory breath hold. Iohexol (Omnipaque 350 mg/mL, GE Healthcare, Buckinghamshire, UK) was administered into an antecubital vein via an 18-gauge intravenous catheter. A volume of 80 to 100 mL at a flow rate of 6 mL/s was used for the image acquisition followed by 50 mL of normal saline.

Images were reconstructed with a slice thickness of 0.6 mm, an increment of 0.5 mm, a temporal resolution of 66 ms and an image matrix of 512×512 pixels. Optimal imaging phases were automatically determined within the ECG trigger window based on the patient's HR and manually adjusted if needed. The selected imaging planes were reconstructed using a medium-soft convolution kernel optimized for vascular imaging with both filtered-back projection (Bv36/Bv40) or iterative reconstruction (SAFIRE or ADMIRE, Siemens Healthcare, Forchheim, Germany at strength level of 3). The effective radiation dose (mSv) was estimated using the dose-length product (DLP) multiplied by a coefficient for the chest as the investigated anatomical region ($\kappa = 0.014$ mSv/mGy*cm) [9].

2.3. Visual CCTA assessment

Image data sets were evaluated on a separate workstation (Syngo Via, Siemens Healthineers, Forchheim, Germany) for visual interpretation. CAC scoring was quantified and expressed in Agatston units and computed using images reconstructed at 3.0 mm slice thickness. High calcium score was defined as CAC ≥ 400 .

Visual analysis was performed by consensus among two physicians including an advanced cardiac imaging fellow and a senior imaging cardiologist with >10 years experience with access to all clinical and imaging data. The coronary artery tree was divided into 18 segments based on established guidelines [10]. Uninterpretable segments were attributed to either extensive calcification or poor visualization. Overall image quality was subjectively assessed at the time of interpretation after consideration of coronary motion,

respiratory motion, image noise and contrast density using a 5-point scale (0 – uninterpretable, 1 – poor, 2 – fair, 3 – good, 4 – excellent). Two examples of study quality assessment are shown in Fig. 1. Good quality studies were classified as those scored as good or excellent.

2.4. Outcomes

The primary outcome was the proportion of scans with uninterpretable coronary segments for any reason. The secondary outcome was the proportion of scans with uninterpretable segments related to calcification and due to poor visualization. Coronary segments with stents were included in the primary and secondary outcome.

2.5. Analysis

Continuous variables were summarized as mean (standard deviation) if normally distributed and compared using a Student's *t*-test. Continuous variables which are not normally distributed were summarized as median (interquartile range) and compared using a Wilcoxon rank-sum test. Categorical variables were summarized as number (proportion) and compared using a Chi-square test or Fisher's Exact test as appropriate.

Our primary analysis compared the proportion of uninterpretable segments stratified by HR at the time of CCTA. Patients with a HR between 50 and 59 at the time of CCTA were used as the reference group. Independent associations with the primary and secondary outcomes were assessed using multivariable logistic regression analysis. Multivariable models included all baseline and imaging variables. Collinearity between factors was assessed with a variance-covariance matrix with no significant collinearity identified. There was a significant interaction between systolic imaging and HR ≥ 90 (interaction adjusted HR 0.07, $p = 0.017$). Therefore, an analysis stratified by acquisition phase was performed. An additional analysis was performed looking at the proportion of major coronary segments (left main, and proximal or mid-left anterior descending, left circumflex or right coronary artery) with uninterpretable segments.

All statistical tests were two-sided, with a p -value <0.05 considered significant. All analyses were performed using Stata version 13 (StataCorp, College Station, Texas). The study was approved by the investigational review board at Cedars-Sinai Medical Center. All patients provided written informed consent and the study protocol conformed with the ethical guidelines of the Declaration of Helsinki.

3. Results

3.1. Baseline demographics

In total, 2620 patients were included, mean age 61.4 ± 12.9 years and 61.2% male. Population characteristics stratified by HR at time of coronary CTA are shown in Table 1. Patients with HR >80 were younger (mean age 56.4, $p < 0.001$ for HR ≥ 90 and 57.2, $p < 0.001$ for HR 80–89 vs. 62.4 for HR 50–59) and more likely to have obesity or diabetes. Only 7 patients had a HR >100 . Patients who were referred from the ER were younger (52.7% vs 62.6%, $p < 0.001$) and less likely to have extensive CAC (7.4% vs. 20.4%, $p < 0.001$).

3.2. Scan interpretability

Uninterpretable segments were present in 229 (8.7%) scans, representing a total of 471 coronary segments. Segments were uninterpretable due to calcium in 123 (4.7%) scans, poor visualization in 84 (3.2%) scans and for both reasons in 22 (0.8%) scans. Fig. 2 shows the proportion of scans with uninterpretable segments according to HR at the time of CCTA. Patients with HR 80–89 (20.3% vs. 8.4%, $p = 0.004$) or HR ≥ 90 (19.4% vs 8.4%, $p = 0.045$) had a higher proportion of scans with any uninterpretable segment. There were similar findings for scans with poorly visualized segments (11.9%, $p = 0.005$ and 16.1%, $p = 0.004$ respectively compared to 3.3%). However, there were no significant differences between groups in the proportion of scans with uninterpretable segments due to calcium.

Univariable and multivariable analyses of the association with scan interpretability are shown in Table 2. In adjusted analyses, HR 80–89 (adjusted OR 4.53, $p < 0.001$) and HR ≥ 90 (adjusted OR 3.05, $p = 0.040$) were associated with an increased likelihood of having a scan with at least one uninterpretable segment. Prior PCI (adjusted OR 3.76, 95% CI 2.33–6.06, $p < 0.001$), and high CAC (adjusted OR 6.63, 95% CI 4.69–9.36, $p < 0.001$) were also associated with an increased likelihood of having a scan with uninterpretable segments.

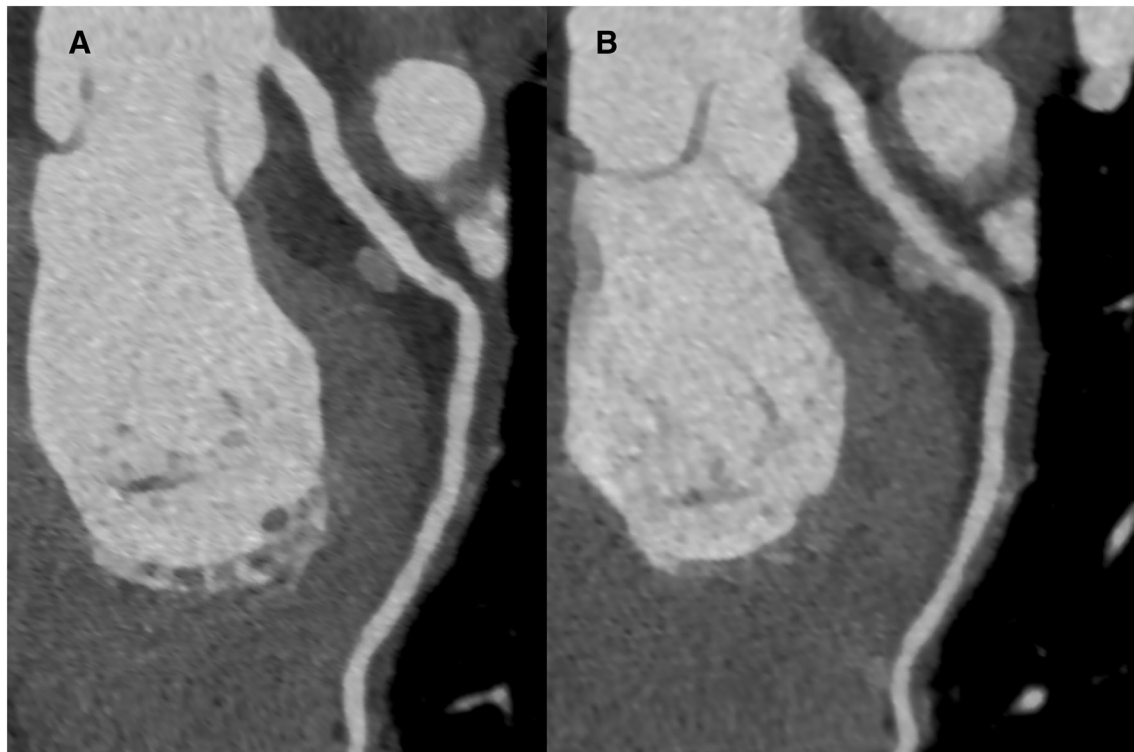


Fig. 1. Examples of study quality assessment. Curved multiplanar reformat of the left circumflex artery in a patient with heart rate of 78. Panel A shows an end-systolic phase (300 msec) which would be classified as “good” quality based on contrast density and lack of significant coronary motion. Panel B shows a mid-diastolic phase (540 msec, ~70%) which would be classified as “fair” quality due to blurring of the proximal, but not distal, segments due to coronary motion.

Supplemental Table 1 outlines the results of multivariable analyses assessing the association with CCTA with poorly visualized segments and segments uninterpretable due to calcium. HR 80–89 (adjusted OR 5.74, 95% CI 2.00–16.5, $p = 0.001$) or HR ≥ 90 (adjusted OR 6.06, 95% CI 1.73–21.2, $p = 0.005$) were associated with an increased likelihood of scans having poorly visualized segments. Increasing HR was not associated with an increased likelihood of scans being uninterpretable due to calcium, but high CAC was (adjusted OR 11.9, 95% CI 7.5–18.7, $p < 0.001$).

Major uninterpretable segments were seen in 127 (4.9%) of scans (65, 2.5% due to calcium; 56, 2.1% due to poor visualization; 6, 0.2% due to both). Univariable and multivariable analysis of the associations with scan interpretability of major coronary segments are shown in the appendix, Supplemental Table 3. HR ≥ 90 (adjusted OR 4.62, 95% CI 1.40–15.3, $p = 0.012$) was associated with an increased likelihood of having a CCTA with at least one uninterpretable major coronary segment.

Table 1
Baseline population characteristics.

	HR <50 N = 440	HR 50–59 N = 1124	HR 60–69 N = 791	HR 70–79 N = 175	HR 80–89 N = 59	HR ≥ 90 N = 31
Age, mean \pm SD	62.0 \pm 12.3	62.4 \pm 12.4	60.7 \pm 13.2	58.7 \pm 14.2	57.2 \pm 13.4	56.4 \pm 18.0
Male, n (%)	314 (71.4)	695 (61.8)	461 (58.3)	87 (49.7)	30 (50.9)	17 (54.8)
BMI, median (IQR)	26.3 (23.7–28.9)	26.5 (24.0–29.7)	26.9 (24.1–30.4)	28.0 (24.5–32.3)	28.5 (24.6–33.4)	26.5 (23.6–31.9)
BMI ≥ 30 kg/m ² , n (%)	79 (18.0)	254 (22.6)	220 (27.8)	61 (34.9)	27 (45.8)	13 (41.9)
Hypertension, n (%)	191 (43.4)	561 (49.9)	417 (52.7)	108 (61.7)	42 (71.2)	19 (61.3)
Diabetes mellitus, n (%)	49 (11.1)	151 (13.4)	128 (16.2)	46 (26.3)	23 (39.0)	13 (41.9)
Dyslipidemia, n (%)	257 (58.4)	742 (66.0)	488 (61.7)	100 (57.1)	28 (47.5)	16 (51.6)
Prior MI, n (%)	26 (5.9)	67 (6.0)	57 (7.2)	13 (7.4)	13 (22.0)	1 (3.2)
Prior PCI, n (%)	35 (8.0)	86 (7.7)	51 (6.5)	14 (8.0)	2 (3.4)	1 (3.2)
Pre-BB HR, median (IQR)	58 (53–67)	62 (58–70)	69 (60–76)	77 (69–85)	86 (79–95)	90 (85–100)
Given beta-blocker, n (%)	224 (50.9)	720 (64.1)	547 (69.2)	143 (81.7)	43 (72.9)	19 (61.3)
Scan HR, median (IQR)	46 (43–48)	55 (52–57)	63 (61–66)	73 (71–75)	84 (81–86)	93 (90–100)
HR variability, median (IQR)	7 (2–16)	4 (2–8)	3 (1–6)	2 (1–4)	2 (1–3)	2 (1–3)
High CAC (≥ 400), n (%)	80 (18.2)	228 (20.3)	138 (17.5)	35 (20.0)	10 (17.0)	8 (25.8)
Prospective imaging, n (%)	239 (86.3)	661 (84.9)	419 (78.5)	62 (50.4)	10 (23.3)	7 (26.9)
Systolic imaging, n (%)	166 (40.7)	460 (42.9)	363 (49.7)	113 (72.0)	42 (79.3)	24 (82.8)
ERD (mSv), median (IQR)	4.3 (2.8–5.9)	4.0 (2.5–5.2)	4.0 (2.5–5.6)	4.8 (2.8–10.0)	6.4 (3.5–11.8)	9.3 (4.3–12.4)
Outpatient, n (%)	356 (80.9)	842 (74.9)	549 (69.4)	100 (57.1)	28 (47.5)	13 (41.9)
Inpatient, n (%)	38 (8.)	142 (12.6)	136 (17.2)	50 (28.6)	25 (42.4)	17 (54.8)
ER patient, n (%)	46 (10.5)	140 (12.5)	106 (13.4)	25 (14.3)	6 (10.2)	1 (3.2)

Baseline population characteristics according to heart rate (HR) at time of coronary computed tomographic angiography. **Bold** denotes statistical significance ($p < 0.05$) compared to HR 50–59. BB – beta-blocker, BMI – body mass index, CAC – coronary artery calcium, ERD – effective radiation dose, HR – heart rate, MI – myocardial infarction, PCI – percutaneous coronary intervention.

3.3. Acquisition phase

There was a significant interaction between systolic imaging and HR ≥ 90 (interaction adjusted HR 0.07, $p = 0.017$). Therefore, an analysis stratified by acquisition phase was performed. Supplemental Fig. 1 shows the proportion of patients with uninterpretable segments, stratified by acquisition phase. There were no significant differences in patients imaged with diastolic acquisition. However, there was a trend towards higher proportion of scans with uninterpretable segments in patients with HR ≥ 90 (40.0 vs. 7.8%, $p = 0.055$). There were no significant differences between HR groups with end-systolic acquisitions.

Multivariable analyses of the association with scan interpretability stratified by phase of acquisition are shown in Supplemental Table 2. With end-systolic acquisition increasing HR was not associated with an increased likelihood of having a scan with uninterpretable segments. However, with diastolic acquisitions HR ≥ 90 (adjusted OR 10.9, 95% CI 1.44–81.5, $p = 0.020$) was associated with an increased likelihood of having a CCTA with uninterpretable segments.

3.4. Image quality and radiation exposure

The majority of scans were acceptable quality (962 [40.9%] excellent and 1166 [49.6%] good). Poor quality, 24 (1.0%) and uninterpretable scans, 10 (0.4%), were uncommon. In unadjusted analysis, HR 70–79 (unadjusted OR 0.55, 95% CI 0.33–0.89, $p = 0.014$), HR 80–89 (unadjusted OR 0.38, 95% CI 0.19–0.76, $p = 0.006$) or HR ≥ 90 (unadjusted OR 0.18, 95% CI 0.08–0.40, $p < 0.001$) were associated with decreased likelihood of having a CCTA with acceptable quality (good or excellent). However, only HR ≥ 90 was associated with a decreased likelihood of acceptable quality in the multivariable analysis (adjusted OR 0.26, 95% CI 0.11–0.63, $p = 0.003$).

There was a weak, but significant, correlation between increasing HR (per 10 beats) and radiation exposure ($r = 0.483$, $p < 0.001$), which was not present after adjusting for baseline demographics and imaging protocol ($r = -0.099$, $p = 0.094$).

4. Discussion

In this large, retrospective cohort study using a third-generation DSCT scanner, patients with HR <80 were not more likely to have an uninterpretable coronary segment compared to patients with HR 50–59. Additionally, the association with uninterpretable coronary segments at a HR >80 was more pronounced with mid-diastolic acquisitions

compared to end-systolic acquisitions. These findings suggest that CCTA remains sufficiently diagnostic at HRs higher than typical guideline thresholds when using third-generation DSCT scanners and end-systolic acquisitions. The implications of this approach on departmental workflow, diagnostic accuracy, and patient satisfaction would need to be tested prospectively.

In our overall population, HR above 80 was associated with a decrease in CCTA interpretability. Nerlekar et al. demonstrated that there was no significant difference in diagnostic accuracy between patients with HRs under 60 compared to patients with a HR from 61 to 80 [11]. Our results build on this evidence by including a larger number of patients, including patients with prior PCI, and assessing all coronary segments. Additionally, although cardiac motion is expected to increase calcium blooming artifact, we did not identify an association between HRs > 80 and segments uninterpretable due to calcium [12]. Finally, increasing HR was correlated with increasing radiation exposure, which was not significant after adjustment for baseline demographics and imaging protocol. However, the larger, multicenter prospective multicenter registry on radiation dose Estimates of cardiac CT angiography in daily practice (PROTECTION VI) study found that each 10 bpm increase is associated with an 8% increase in radiation exposure [13]. Therefore, imaging centers with third-generation DSCT scanners may be able to switch to a HR goal of <80 without impacting image quality or interpretation, but at the expense of slightly higher radiation exposure.

Although HR ≥ 80 was associated with an increased likelihood of scans having uninterpretable segments, this finding was less prominent with end-systolic acquisitions. Our results add to a growing body of evidence that image quality can be improved with end-systolic acquisitions at HRs ≥ 80 . Studies have suggested that cardiac motion was less prominent in systolic imaging of high HRs compared to diastolic imaging [6,14,15]. Lee et al. showed that HR was not correlated with motion artifacts in patients undergoing systolic imaging but was in patients with diastolic imaging [16]. In a study by Chung et al., cardiac diastasis was essentially absent at HRs above 96 bpm [4]. It is possible that systolic imaging in combination with intracycle motion-correction algorithms provides adequate imaging in even higher HRs [17,18]. We also showed that HR variability was not associated with image interpretability in patients imaged with end-systolic acquisitions. This agrees with previous studies suggesting that systolic imaging may improve image quality and diagnostic confidence in patients with atrial fibrillation [19,20]. Our study shows that end-systolic imaging should be preferred first-line technique in patients with either increased HR or HR variability.

The major clinical implication of our finding is that patients with a resting HR under 80 may not require beta-blockade. Notably, we did not find any significant associations between pre-scan beta-blocker administration and image interpretability in adjusted analysis. Over 80% of our patient population had a HR under 80, so this could potentially greatly improve departmental workflow. Benefits may be even greater for patients referred from the ER, of whom over 90% had a HR under 80, since pre-scan beta-blockade adds directly to total ER time. Given the impact of beta-blockade on resting HR and HR variability [21], prospective studies would be needed to confirm this finding.

Our study has a few important limitations. Image acquisition type and phase of acquisition were not controlled prospectively, and patient factors likely affected selection. However, previous studies have shown that the diagnostic accuracy of prospective imaging is comparable to helical acquisitions in patients with high HRs [22]. Additionally, we did not perform manual review of scans to verify motion artifact or assess feasibility of quantitative plaque analysis. However, our results are reflective of routine clinical interpretation of images. We did not account for specific cardiac rhythms that may impact image quality, such as atrial fibrillation, but we did quantify HR variation. Finally, the number of patients with HRs over 80 was relatively small. Therefore, larger studies will be needed to exclude small differences in image interpretability at high HRs with end-systolic acquisitions.

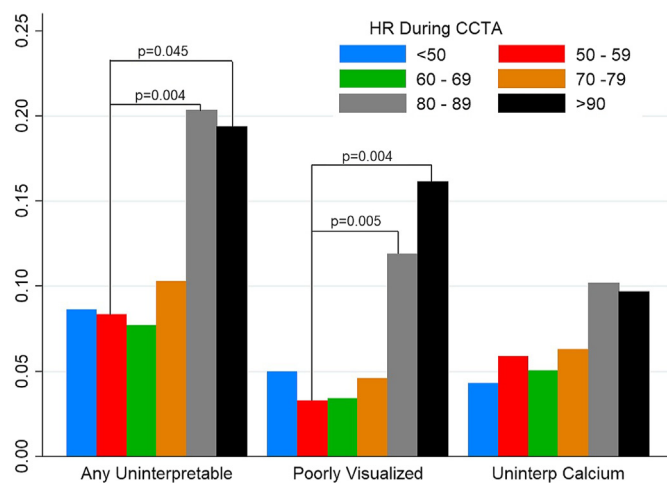


Fig. 2. Proportion of scans with any uninterpretable segments stratified by heart rate at time of scan. Heart rate (HR) at time of coronary computed tomographic angiography (CTA) 50–59 used as reference group, significant values as shown.

Table 2
Associations with scans showing any uninterpretable segments.

	Univariable analysis		Multivariable analysis	
	Unadjusted OR (95% CI)	P-value	Adjusted OR (95% CI)	p-Value
Age (per year)	1.05 (1.03–1.07)	<0.001	1.02 (1.00–1.04)	0.024
Male	1.92 (1.41–2.61)	<0.001	1.38 (0.95–1.99)	0.092
BMI ≥ 30 kg/m ²	1.36 (1.01–1.83)	0.041	1.25 (0.84–1.87)	0.277
Hypertension	2.50 (1.86–3.36)	<0.001	1.40 (0.97–2.01)	0.070
Diabetes mellitus	2.41 (1.77–3.28)	<0.001	1.26 (0.86–1.85)	0.231
Dyslipidemia	1.55 (1.15–2.09)	0.004	1.10 (0.77–1.57)	0.614
Prior MI	2.00 (1.29–3.08)	0.002	0.67 (0.37–1.20)	0.179
Prior PCI	5.50 (3.88–7.79)	<0.001	3.76 (2.33–6.06)	<0.001
Given BB	1.45 (1.07–1.96)	0.016	1.27 (0.89–1.82)	0.186
HR variability	1.14 (1.03–1.26)	0.010	1.10 (0.98–1.25)	0.115
High CAC (≥400)	9.93 (7.4–13.3)	<0.001	6.63 (4.69–9.36)	<0.001
Prospective	0.65 (0.48–0.88)	0.005	0.94 (0.62–1.45)	0.791
Systolic	1.16 (0.88–1.54)	0.287	1.02 (0.74–1.41)	0.910
Location – reference outpatient				
Inpatient	0.96 (0.67–1.39)	0.839	1.20 (0.77–1.88)	0.422
ER patient	0.27 (0.14–0.53)	<0.001	0.42 (0.18–0.96)	0.041
HR – reference 50–59				
HR <50	1.04 (0.70–1.54)	0.861	1.03 (0.66–1.62)	0.886
HR 60–69	0.92 (0.65–1.28)	0.607	1.06 (0.76–2.60)	0.276
HR 70–79	1.26 (0.74–2.14)	0.400	1.41 (0.76–2.60)	0.276
HR 80–89	2.80 (1.43–5.46)	0.003	4.53 (2.02–10.2)	<0.001
HR ≥ 90	2.63 (1.05–6.57)	0.038	3.05 (1.05–8.85)	0.040

Association between variables and scans with uninterpretable segments (poorly visualized or due to calcification). BB – beta-blocker, BMI – body mass index, CABG – coronary artery bypass grafting, CAC – coronary artery calcium, HR – heart rate, MI – myocardial infarction, PCI – percutaneous coronary intervention.

5. Conclusions

With third-generation DSCT scanners, patients with a HR under 80 can be imaged without impairing scan interpretability. HR over 80 continues to be associated with impairment in CCTA image interpretability. However, the association with uninterpretable coronary segments at HRs > 80 was less prominent with end-systolic imaging. Imaging centers with third-generation DSCT scanners may be able to switch to a HR goal of <80 without impacting image quality or interpretation and potentially higher if systolic imaging is used routinely.

Supplementary data to this article can be found online at <https://doi.org/10.1016/j.ijcard.2019.07.098>.

Funding

The work was supported in part by the Miriam and Sheldon G. Adelson Medical Research Foundation. Dr. Miller receives salary support from the Arthur JE Child Fellowship grant.

Conflicts of interest

The authors have no relevant conflicts of interest to disclose.

Acknowledgements

None.

References

- [1] U. Hoffmann, Q.A. Truong, D.A. Schoenfeld, E.T. Chou, P.K. Woodard, J.T. Nagurney, et al., Coronary CT angiography versus standard evaluation in acute chest pain, *N. Engl. J. Med.* 367 (4) (2012) 299–308.
- [2] C. Hamilton-Craig, A. Fifoot, M. Hansen, M. Pincus, J. Chan, D.L. Walters, et al., Diagnostic performance and cost of CT angiography versus stress ECG—a randomized prospective study of suspected acute coronary syndrome chest pain in the emergency department (CT-COMPARE), *Int. J. Cardiol.* 177 (3) (2014) 867–873.
- [3] D.E. Newby, P.D. Adamson, C. Berry, N.A. Boon, M.R. Dweck, M. Flather, et al., Coronary CT angiography and 5-year risk of myocardial infarction, *N. Engl. J. Med.* 379 (10) (2018) 924–933.
- [4] C.S. Chung, M. Karamanoglu, S.J. Kovacs, Duration of diastole and its phases as a function of heart rate during supine bicycle exercise, *Am. J. Physiol. Heart Circ. Physiol.* 287 (5) (2004) H2003–H2008.
- [5] S. Abbara, P. Blanke, C.D. Maroules, M. Cheezum, A.D. Choi, B.K. Han, et al., SCCT guidelines for the performance and acquisition of coronary computed tomographic angiography: a report of the Society of Cardiovascular Computed Tomography Guidelines Committee: Endorsed by the North American Society for Cardiovascular Imaging (NASCI), *J. Cardiovasc. Comput. Tomogr.* 10 (6) (2016) 435–449.
- [6] H. Brodoefel, A. Reimann, M. Heuschmid, A. Küttner, T. Beck, C. Burgstahler, et al., Non-invasive coronary angiography with 16-slice spiral computed tomography: image quality in patients with high heart rates, *Eur. Radiol.* 16 (7) (2006) 1434–1441.
- [7] F. Cademartiri, N.R. Mollet, G. Runza, M. Belgrano, P. Malagutti, B.W. Meijboom, et al., Diagnostic accuracy of multislice computed tomography coronary angiography is improved at low heart rates, *Int. J. Card. Imaging* 22 (1) (2006) 101–105.
- [8] A.S. Agatston, W.R. Janowitz, F.J. Hildner, N.R. Zusmer, M. Viamonte, R. Detrano, Quantification of coronary artery calcium using ultrafast computed tomography, *J. Am. Coll. Cardiol.* 15 (4) (1990) 827–832.
- [9] The 2007 Recommendations of the International Commission on Radiological Protection, ICRP publication 103, *Annal ICRP* 37 (2–4) (2007) 1–332.
- [10] J. Leipsic, S. Abbara, S. Achenbach, R. Cury, J.P. Earls, G.J. Mancini, et al., SCCT guidelines for the interpretation and reporting of coronary CT angiography: a report of the Society of Cardiovascular Computed Tomography Guidelines Committee, *J. Cardiovasc. Comput. Tomogr.* 8 (5) (2014) 342–358.
- [11] N. Nerlekar, B.S. Ko, A. Nasis, J.D. Cameron, M. Leung, A.J. Brown, et al., Impact of heart rate on diagnostic accuracy of second generation 320-detector computed tomography coronary angiography, *Cardiovasc. Diagn. Ther.* 7 (3) (2017) 296–304.
- [12] P. Li, L. Xu, L. Yang, R. Wang, J. Hsieh, Z. Sun, et al., Blooming artifact reduction in coronary artery calcification by a new de-blooming algorithm: initial study, *Sci. Rep.* 8 (1) (2018) 6945.
- [13] T.J. Stocker, S. Deseive, J. Leipsic, M. Hadamitzky, M.Y. Chen, R. Rubinshtein, et al., Reduction in radiation exposure in cardiovascular computed tomography imaging: results from the PROspective multicenter registry on radiation dose Estimates of cardiac CT angIOgraphy iN daily practice in 2017 (PROTECTION VI), *Eur. Heart J.* 39 (41) (2018) 3715–3723.
- [14] H. Seifarth, S. Wienbeck, M. Püsken, K.-U. Juergens, D. Maintz, C. Vahlhaus, et al., Optimal systolic and diastolic reconstruction windows for coronary CT angiography using dual-source CT, *Am. J. Roentgenol.* 189 (6) (2007) 1317–1323.
- [15] P.A. Araoz, J. Kirsch, A.N. Primak, N.N. Braun, O. Saba, E.E. Williamson, et al., Optimal image reconstruction phase at low and high heart rates in dual-source CT coronary angiography, *Int. J. Cardiovasc. Imaging* 25 (8) (2009) 837–845.
- [16] A.M. Lee, J. Beaudoin, L.-C. Engel, M.S. Sidhu, S. Abbara, T.J. Brady, et al., Assessment of image quality and radiation dose of prospectively ECG-triggered adaptive dual-source coronary computed tomography angiography (cCTA) with arrhythmia rejection algorithm in systole versus diastole: a retrospective cohort study, *Int. J. Cardiovasc. Imaging* 29 (6) (2013) 1361–1370.
- [17] Z.-N. Li, W.-H. Yin, B. Lu, H.-B. Yan, C.-W. Mu, Y. Gao, et al., Improvement of image quality and diagnostic performance by an innovative motion-correction algorithm for prospectively ECG triggered coronary CT angiography, *PLoS One* 10 (11) (2015), e0142796.
- [18] Cho I, Elmore K, Ó Hartaigh B, Schulman-Marcus J, Granser H, Valenti V, et al. Heart-rate dependent improvement in image quality and diagnostic accuracy of coronary computed tomographic angiography by novel intracycle motion correction algorithm. *Clin. Imaging* 2015 2015 May–Jun;39(3):421–6.

- [19] M.B. Srichai, M. Barreto, R.P. Lim, R. Donnino, J.S. Babb, J.E. Jacobs, Prospective-triggered sequential dual-source end-systolic coronary CT angiography for patients with atrial fibrillation: a feasibility study, *J. Cardiovasc. Comput. Tomogr.* 7 (2) (2013) 102–109.
- [20] B. Clayton, C. Roobottom, G. Morgan-Hughes, CT coronary angiography in atrial fibrillation: a comparison of radiation dose and diagnostic confidence with retrospective gating vs prospective gating with systolic acquisition, *Br. J. Radiol.* 88 (1055) (2015), 20150533.
- [21] G. Sandrone, A. Mortara, D. Torzillo, M.T. La Rovere, A. Malliani, F. Lombardi, Effects of beta blockers (atenolol or metoprolol) on heart rate variability after acute myocardial infarction, *Am. J. Cardiol.* 74 (4) (1994) 340–345.
- [22] H.Y. Kim, J.W. Lee, Y.J. Hong, H.-J. Lee, J. Hur, J.E. Nam, et al, Dual-source coronary CT angiography in patients with high heart rates using a prospectively ECG-triggered axial mode at end-systole, *Int. J. Cardiovasc. Imaging* 28 (2) (2012) 101–107.